

Theoretical analysis of the synergism in the dielectric strength for SF₆/CF₄ mixtures

A. V. Larin

Laboratoire de Physico-Chimie Informatique, Facultés Universitaires Notre-Dame de la Paix, Rue de Bruxelles 61, B-5000 Namur, Belgium and Laboratory of Molecular Beams, Department of Chemistry, Moscow State University, Leninskie Gory, Moscow, B-234, 119899, Russia

N. Meurice

Laboratoire de Physico-Chimie Informatique, Facultés Universitaires Notre-Dame de la Paix, Rue de Bruxelles 61, B-5000 Namur, Belgium

D. N. Trubnikov

Laboratory of Molecular Beams, Department of Chemistry, Moscow State University, Leninskie Gory, Moscow, B-234, 119899, Russia

D. P. Vercauteren^{a)}

Laboratoire de Physico-Chimie Informatique, Facultés Universitaires Notre-Dame de la Paix, Rue de Bruxelles 61, B-5000 Namur, Belgium

(Received 10 November 2003; accepted 29 March 2004)

Available cross section data of electron–molecule processes are scaled to simulate the behavior of the dielectric strength (DS) in SF₆ and CF₄ gases at the level of the two-term approximation of the Boltzmann equation solution corresponding to the homogeneous electric field model. Then, the DS of mixtures is evaluated and compared to experimental data. The reasons of the synergism and its “asymmetry” relative to both components in SF₆/CF₄ mixtures are analyzed in terms of rate constant variations with respect to their values for the pure gases as well as in terms of weighted rate constants for all channels of electron energy losses relevant under breakdown conditions. © 2004 American Institute of Physics. [DOI: 10.1063/1.1751637]

I. INTRODUCTION

Environmental impacts related to the global warming potential (GWP) and ozone depletion potential (ODP) limit future applications of the most popular dielectric gas, SF₆, and therefore initiate new fields for searching new potent candidates. Towards these goals, several technical conditions as the low dew point, the high dielectric strength (DS), together with environmental requirements, suggest the consideration of gas mixtures rather than pure gases. Then, an important condition for the use of mixtures is the optimal ratio of each component which could lead to the highest DS relative to the average value of the pure components. More precisely, this situation, described by the term “synergism,” corresponds to mixture compositions whose DS value at any content is simply larger than the value obtained by the linear interpolation between the values of the two isolated gases. In this study, we shall limit ourselves to the case of synergism only, not touching the “positive synergism” effect in the DS as proposed by Hunter and Christophorou,¹ namely, that a maximum condition (i.e., the derivative of the DS with respect to the mixture composition is equal to zero) has to be satisfied at least for one particular content of the mixture and that the DS value is always larger than the DS values of the two isolated components at the particular content. As shown in Ref. 1, a positive synergism is assigned to an increase of anionic stability with respect to electron detachment owing

to a series of secondary ion exchange reactions. This idea was proven experimentally by the analysis of current waves under small pressures, for example, for mixtures of *c*-C₄F₈ and 1-C₃F₆, for which electron and ionic currents were recorded separately, which confirmed the hypothesis.²

While the rare positive synergism situations have been explained, the mechanisms of synergism which has been more frequently observed have, to our best knowledge, not yet been clearly analyzed and the reasons of the phenomenon have not yet been clearly explained. Several analyses were proposed for quasi ideal cases, e.g., when a relatively full set of information about the cross sections (CSs) of the various electron–molecule processes is available for both components. In such cases, it is indeed possible to evaluate reliably the DS increase coming from the variations of the electron energy losses between the possible channels in the pure gases compared to the ones in their mixtures. For example, for SF₆/N₂ mixtures the importance of the influence of vibrational relaxation, considering attachment coefficients of the mixture and different models of N₂ vibrational levels, on the electron energy decrease was clearly shown.³ To the light of updated CSs for both the CF₄ (Ref. 4) and SF₆ (Ref. 5) gases, analyses of the “microscopic” partition of the electron energy losses at the breakdown limit could thus explain, as first goal, the synergism of the DS in the case of their mixtures.

Three different approaches can principally be considered for the simulation of the behavior of the DS for gas mixtures, i.e., a graphical or “phenomenological” method,^{6,7} the Bolt-

^{a)}Author to whom correspondence should be addressed.

zmann equation (BE) solution under two-term^{3,8,9} or three-term^{10–12} approximations, and Monte Carlo simulations.¹³ The easiest evaluations can be performed using the phenomenological method proposed by Wieland.⁶ This graphical solution requires the knowledge of the ionization and attachment coefficients with respect to the reduced electric field E/N . It should however be mentioned that the graphical method is of lower precision and reliability as compared to the BE solution. It cannot neither give a physical interpretation of the reasons of the increase of the DS for the mixtures with respect to the ideal linear behavior between the two values of the two individual gases and thus cannot really help in future studies of candidate mixtures.

In our work, we evaluated the DS increase owing to the synergism at the level of the BE solution, i.e., accurate scaled CSs were applied for the BE solution within two-term decompositions of the electron energy distribution functions. Then the rate constants for pure gases were evaluated and their changes were compared to the ones in SF₆/CF₄ mixtures exposed to the same E/N fields. First, a DS fitting of the experimental DS value of the pure gases was realized based on the coincidence between the experimental and calculated attachment and ionization coefficients as well as of the drift velocities with respect to E/N . As an additional tool, we analyzed the weighted rate constants for the mixtures which allowed us to conclude on what the favored channels are for the mixtures at the breakdown limit.

In Sec. II, we describe the theoretical aspects of the chosen model and explain our choice of computational code. Section III A is devoted to the available CS data for SF₆ and CF₄ as well as to the fitting of the CSs for both gases via the comparison of the known experimental ionization, attachment, dielectric strength, and drift velocity. In Sec. III B, we discuss the calculation of the DS for several compositions of SF₆/CF₄ mixtures using the BE method and compare the results of the BE solution to the known experimental data. The variations of the rate constants via the different channels relative to their values for the pure gas are compared and the reasons of the asymmetric position of the DS “maximum” in the mixtures are discussed.

II. THEORETICAL AND COMPUTATIONAL ASPECTS

Addressing the question of electron–molecule collision processes under relatively high reduced electric fields, we choose the first-order (two-term approximation) decomposition of the electron energy distribution function for the solu-

tion of the Boltzmann transport equation. For CF₄, the differences between the solutions at the first and second (three-term) order levels were shown to be related to small reduced E/N values.¹⁴ For SF₆, no visible difference was shown for E/N values ranging from 150 to 700 Td.¹¹ Hence, in order to avoid the problem of high elastic/inelastic collision ratios under such conditions which are particularly important for CF₄, the two-term BE solutions are not recommended at small E/N values, i.e., for CF₄ and its mixtures, not lower than 100 Td,¹⁴ for SF₆ and its mixtures, not lower than 100–150 Td.¹²

Within the framework of the BE solution, the CSs are required for both mixture components. It means that a scaling procedure varying several chosen CSs is necessary to fit the experimental data,¹² even for such a well studied gas as SF₆ irrespective of the computational method. Different ways to scale the CSs have already been proposed in the literature, mainly combining a direct multiplication of the separate CSs, conserving their dependence vs the energy of the electrons, with local modifications of the momentum transfer CS.^{11,15} More complicated procedures consisting in a four-step fitting of the different CSs, related to the specific BE method used by the authors in Ref. 12, have also been proposed but their adoption cannot be conjugated with our tools. We hence chose the first mentioned method.

The complete study of any system, individual gases or mixtures, *a priori* requires a simultaneous kinetic solution of all decomposition reactions. However, an important problem is that all the CSs for all the degradation radical products of the reaction are not known and thus the precise calculation of the electron swarm parameters becomes difficult. Performing all calculations at standard temperature and pressure, we decided to solve the problem under the hypothesis that the concentrations of the reaction products are small as compared to the nearly constant concentration of the SF₆ and CF₄ gases at dielectric breakdown condition, sharing the same basic model as applied for SF₆ mixtures with Ne and O₂ by Phelps and Van Brunt.¹⁵ This is justified by the small ionic concentration under normal breakdown conditions.¹⁶

The parameters that need to be controlled are the electron swarm parameters, i.e., the:

- (1) drift velocities

$$\nu = -\frac{1}{3} \sqrt{\frac{2eE}{mN}} \int_0^\infty \frac{1}{\sum_s \delta_s(\varepsilon) \sigma_s(\varepsilon)} \times \frac{df_0}{d\varepsilon} \varepsilon d\varepsilon, \quad (1)$$

where σ_s is the moment transfer CS of s component, δ_s ,

TABLE I. Scaling of the literature parameters of the different cross sections, variation of the reduced electric field $(E/N)_{cr}$ or dielectric strength variation (DSV) (%) with respect to a 20% decrease of the scaling factor.

Gas	$(E/N)_{cr}$ Td	Momentum transfer	Vibration (direct/indir.)	Attachment /diss. attach.	Ionization	Dissociation into neutrals
CF ₄ (set 1)	143.5	0.9	0.36/0.35	1.3/...	1.2	1.0
DSV (set 1)	0./–6.5%	–4.1%	+1.1%	–1.3%
CF ₄ (set 2)	140.0	1.0	0.36/0.36	1.0/...	2.2	1.0
SF ₆ (set 1)	360.1	0.6	1.0	1.3/1.3	2.3	1.2
DSV (set 1)	0.0%	0.0%	+5.5%	–9.0%
SF ₆ (set 2)	361.6	0.7	1.0	1.15/1.15	2.0	1.0

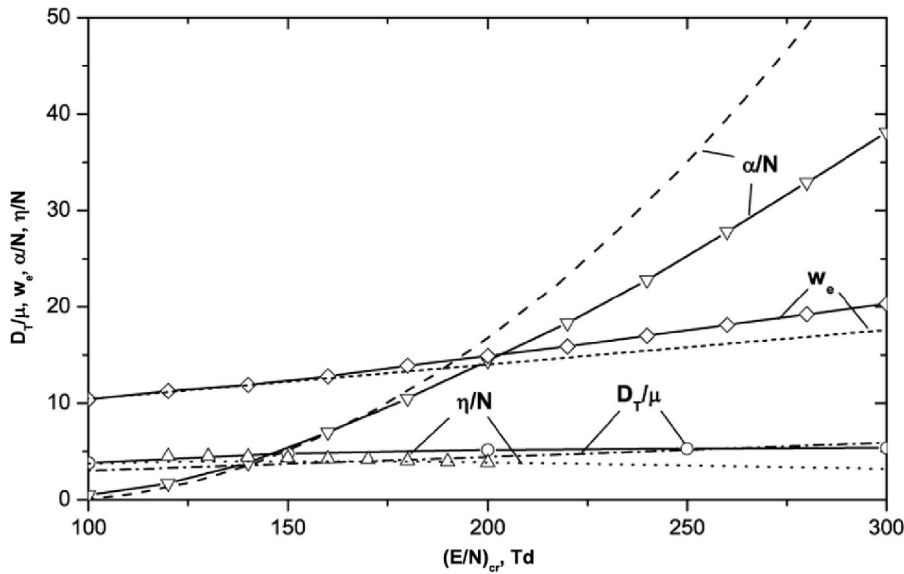


FIG. 1. Experimental (Ref. 4) (solid lines and symbols) reduced attachment η/N (in 10^{-16} cm², triangles up), reduced ionization α/N (in 10^{-16} cm², triangles down), electron drift velocity w_e (in 10^6 cm/s, diamonds), ratio of transverse electron diffusion coefficient to electron mobility D_T/μ (in 10^{-1} V, circles) and calculated η/N (dotted line), α/N (dashed line), w_e (short dashed line), D_T/μ (dotted-dashed line) vs the reduced electric field (Td) for the chosen CS set 1 from Table I for CF₄.

the molar fraction of s component, f_0 , the zero approximation to the electron energy distribution function $f(\mathbf{v}) = f_0(v) + (\mathbf{v}/v)f_1$ (\mathbf{v} being the electron velocity vector), and E/N , the reduced electric field;

(2) rate constants in the j process of the s component

$$k_{sj} = \sqrt{\frac{2e}{m}} \int_0^\infty \sigma_{sj}(\epsilon) f(\epsilon) \epsilon \, d\epsilon, \quad (2)$$

where σ_{sj} is the CS of s component in the j process;

(3) diffusion coefficients

$$D = \frac{1}{3N} \sqrt{\frac{2e}{m}} \int_0^\infty \frac{1}{\sum_s \delta_s(\epsilon) \sigma_s(\epsilon)} f(\epsilon) \epsilon \, d\epsilon. \quad (3)$$

In the present work, the diffusion coefficient will be compared to the experimental D_T/μ values, wherein the electron mobility is $\mu = v/E$, v being the electron drift velocities.

The proposed scheme for the fitting of the scaling factors was determined by the necessity to reproduce the DS values,

first for the pure gases and then for their mixtures:

- (1) Variation of the scaling factors to first agree with the experimental breakdown values. Testing of the DS response with respect to the CS variations in order to reveal the most important or “sensitive” CSs;
- (2) Empirical changes of the scaling factors of the CSs to fit the experimental drift velocities and/or rate constants for the pure gas while conserving the experimental breakdown values.

Among three available computing codes,^{17–19} the NOMAD (Ref. 18) and ELENDIF (Ref. 19) programs present similar possibilities and both include electron attachment processes which are not considered in BOLTZ.¹⁷ Because NOMAD is more restricted by available energies of electron–electron collisions as compared to ELENDIF, we chose the latest code.

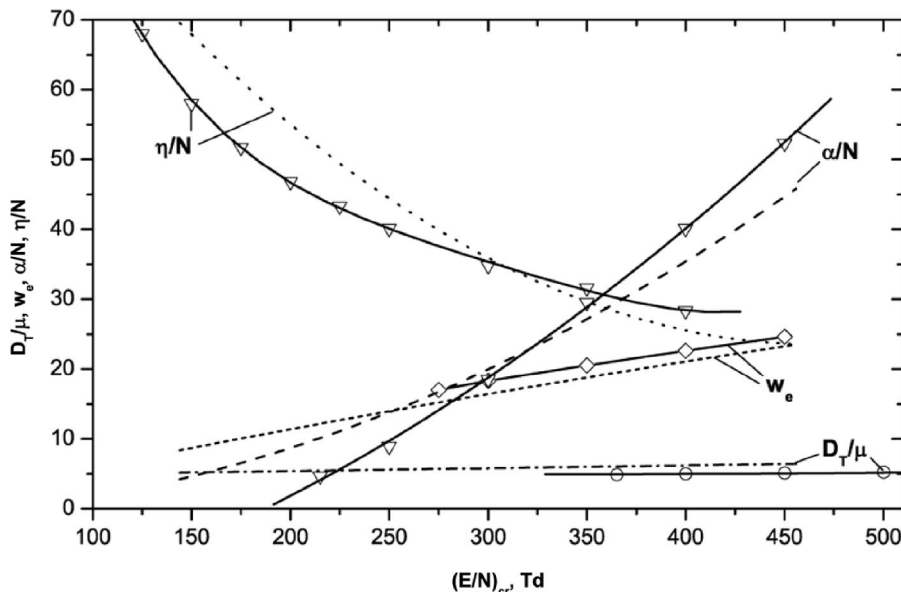


FIG. 2. Experimental (Ref. 5) (solid lines and symbols) reduced attachment η/N (in 10^{-16} cm², triangles up), reduced ionization α/N (in 10^{-16} cm², triangles down), electron drift velocity w_e (in 10^6 cm/s, diamonds), ratio of transverse electron diffusion coefficient to electron mobility D_T/μ (in 10^{-1} V, circles) and calculated η/N (dotted line), α/N (dashed line), w_e (short dashed line), D_T/μ (dotted-dashed line) vs the reduced electric field (Td) for chosen CS set 1 from Table I for SF₆.

TABLE II. Comparison between the calculated and experimental electron swarm parameters at the breakdown conditions ($P=1$ atm, $T=300$ K) and reduced electric field $(E/N)_{cr}$.

Gas	$(E/N)_{cr}$, Td	Reduced mean energy, eV	Characteristic energy, V	Attachment rate constant, $\times 10^{-10}$ cm ³ /s	Drift velocity, $\times 10^{-7}$ cm/s
CF ₄ (set 1)	143.5	2.919	3.618	0.418	1.208
CF ₄ (set 2)	139.9	2.739	3.436	0.350	1.104
Expt. ^a	140	...	2.41	0.526	1.190
		(From e-energy)		0.3–0.4	...
SF ₆ (set 1)	360.1	5.189	6.033	4.145	1.925
SF ₆ (set 2)	358.0	5.189	6.046	4.764	1.638
Expt. ^b	350	...	4.86	6.478	2.05

^aReference 4.^bReference 5.

For convenience, we interfaced ELENDF (Ref. 19) to the RTBIS subroutine²⁰ in order to facilitate the determination of the breakdown value via a bisection method. A correction was also done in the main subroutine FDIFF of ELENDF.²¹ The calculated scaling parameters of the different CSs are presented in Table I.

Let us mention that no particular electrode geometry can be used for the determination of the breakdown criterion in the case of an uniform field treated with the BE method as implemented in ELENDF.¹⁹ Hence, for electronegative gases the problem of the DS calculation is reduced to the steady state approximation for the determination of the breakdown point, i.e., the velocity of the electrons production owing to the ionization processes is equal to the velocity of the electron attachment in the system. This criterion could be chosen as the two gas components, SF₆ and CF₄, are electronegative gases. This simplified solution can also be applied for mixtures of gases with a dominating concentration of the electronegative component. For each gas, all the ionization processes were considered as a unified channel with one CS value only. The same approximation was done for all the attachment processes.

III. RESULTS

A. Fitting of the cross sections for individual components

First, we present the general trends for both gases, such as the minor importance of the rotational CSs at the breakdown conditions irrespective of the continuous approximation or numerical input²⁰ of the rotational CS; hence it is omitted in the following discussion.

Although CF₄ is one of the most studied molecule, several problems can appear even at the most accurate computational level as compared to the two-term approximation applied herein. For example, independently assessed CSs for this gas²² (i.e., independent sources, thus without fitting) led to a worse agreement with the experimental ionization coefficient as compared to the application of the CSs fitted with the BE solution.¹⁴ As soon as the CSs fitted with the BE solution are not available, independent CSs were however used in our work. This solution led to accurate experimental ionization values at the breakdown of pure CF₄ but overestimated ionizations were observed at reduced field values

higher than 160–170 Td (Fig. 1). Comparison with available experimental data for individual gases are shown in Figs. 1, 2 and Table II. The calculated electron drift velocities are only slightly underestimated for both gases but keep correct ratio between them within all the required range of E/N values. That is important for the variation of the electron energy distribution function (EEDF) vs the mixture ratio variation. Transverse diffusion coefficients are slightly underestimated for CF₄ (below 250 Td) and overestimated for SF₆. We can say that we obtained a qualitative correct behavior of the calculated properties for both components, which allowed to pass to the next step, the simulations of the mixtures.

In order to reveal the most sensitive CSs and thus to accelerate the fitting by scaling these most important ones, we evaluated the variation of the calculated critical $(E/N)_{cr}$ value with respect to a 20% decrease of the chosen CSs with exception of the momentum transfer CS which is evidently very important (Table I). For CF₄, the variations showed a particular strong DS dependence on the vibrational indirect excitations, i.e., owing to electron-vibrational interactions of several vibrational modes. This CS is thus in essential extent a hidden “electron excitation” CS. In order to evaluate the importance of each channel of the electron energy losses at the breakdown conditions, we compared the weighted rate constants (Table III). In the case of SF₆, the dissociation into neutral particles CS was evaluated as the most important for the DS change. One should note that the dominations of these channels were also observed for the mixture.

B. Calculation of the dielectric strength for the SF₆/CF₄ mixtures with the Boltzmann method

In order to achieve the breakdown dependence vs the gas contents, we determined the $(E/N)_{cr}$ values on a grid by step

TABLE III. Weighted rate constants at the breakdown conditions ($P=1$ atm, $T=300$ K) and reduced electric field $(E/N)_{cr}$.

Gas	$(E/N)_{cr}$, Td	Vibration loss, %	Attachment loss, %	Ionization loss, %	Dissociation into neutrals loss, %
CF ₄ (set 1)	143.5	90.9	1.8	4.2	3.0
SF ₆ (set 1)	360.1	2.7	0.004	12.1	82.1

TABLE IV. Calculated relative dielectric strength (DS) increase and reduced electric field $(E/N)_{cr}$ values in the SF_6/CF_4 mixture.

% SF_6	0	10	20	30	40	50	60	70	80	90	100
% DS	0	12.7	14.9	14.5	12.9	11.1	8.6	6.4	4.2	2.1	0.0
$(E/N)_{cr}$	143.5	186.1	214.7	238.6	259.7	279.0	297.0	313.9	330.0	345.3	360.1

of 10%. Results of the calculations for the mixture are given in Table IV and Fig. 3. The calculated maximum corresponds to a 14.9% increase relative to the mean value of the pure gases at 20 mol % of SF_6 . A direct comparison with experimental results for SF_6/CF_4 (Refs. 25 and 26) is not possible as numerical DS data are not available; we only have experimental confirmation of the synergism. The presence of corona stabilization effects in the experimental data cannot neither be ignored at large gaps between the electrodes in strongly nonuniform field,²⁶ which did not allow to evaluate more precisely the respective SF_6 content at which the DS has a “maximum.” But at small electrode gaps it is clear from the figures in Ref. 26 that the optimal SF_6 content obtained upon studies corresponds to less than 50% of SF_6 .

Numerical data extracted from Paschen curves are available for a close mixture, i.e., SF_6/CHF_3 .²³ The absence of $(E/N)_{cr}$ values for pure CHF_3 does not allow to evaluate the synergism in this mixture. The value expressed in Ref. 23 via $(E/P)_{lim}$, P being the gas pressure, was resolved by using a ninth-order polynomial extrapolation over 12 experimental points ranging between 5% and 100%. Thus the $(E/P)_{lim}$ of pure CHF_3 was estimated as 3.25 kV/mm/bar which allowed to evaluate the synergism in the SF_6/CHF_3 mixture. After this, the synergism was adapted to our Townsend (Td) scale (Fig. 3) and compared in Table V with the one calculated for the SF_6/CF_4 mixture (Table IV) considering that $DS(SF_6) = 360.1$ Td and $DS(CHF_3) = 128.9$ Td.²⁴ Experiment showed a slightly higher increase up to 19.9% at the same content of 20 mol % for SF_6/CHF_3 as calculated herein for

SF_6/CF_4 . This coincidence in the maximum position and the closeness to the calculated DS increase of 14.6% validate the computational results. One should note that the synergism is observed at nearly the same gas content as for SF_6/N_2 , i.e., 20 mol % of SF_6 .⁷

In order to analyze the reasons of the DS increase (synergism) in the mixture, we considered several variations of the weighted rate constants (WRC) w_{sj} of the different channels of electron energy losses (Fig. 4):

$$w_{sj} = \frac{k_{sj} \epsilon_{sj} \rho_{sj} \delta_s}{\sum_{s,j} k_{sj} \epsilon_{sj} \rho_{sj} \delta_s}, \tag{4}$$

where δ_s , k_{sj} , ρ_{sj} , ϵ_{sj} are the fraction of the s component, rate constant, occupation of the lowest state, and energy threshold of the j channel for each s component, respectively. It is important to note that the ϵ_{sj} values in Fig. 4 are shown with respect not only to $(E/N)_{cr}$, but also to the respective mixture SF_6/CF_4 content which varies together with the abscissa in accordance with the data from Table IV.

Both the dissociation into neutral particles (DN) of SF_6 and ionization are characterized by high WRC values for both components [Fig. 4(b)]. In terms of the w_{ij} constants, all ranges of concentrations can be partitioned into two parts. The first, at small SF_6 concentrations, is “controlled” owing to the increased effectiveness of the vibrational indirect excitations relative to pure CF_4 , while the second domain, at high SF_6 concentrations, is governed by the DN channel of SF_6 . In the case of the SF_6/CF_4 mixture, these two energy

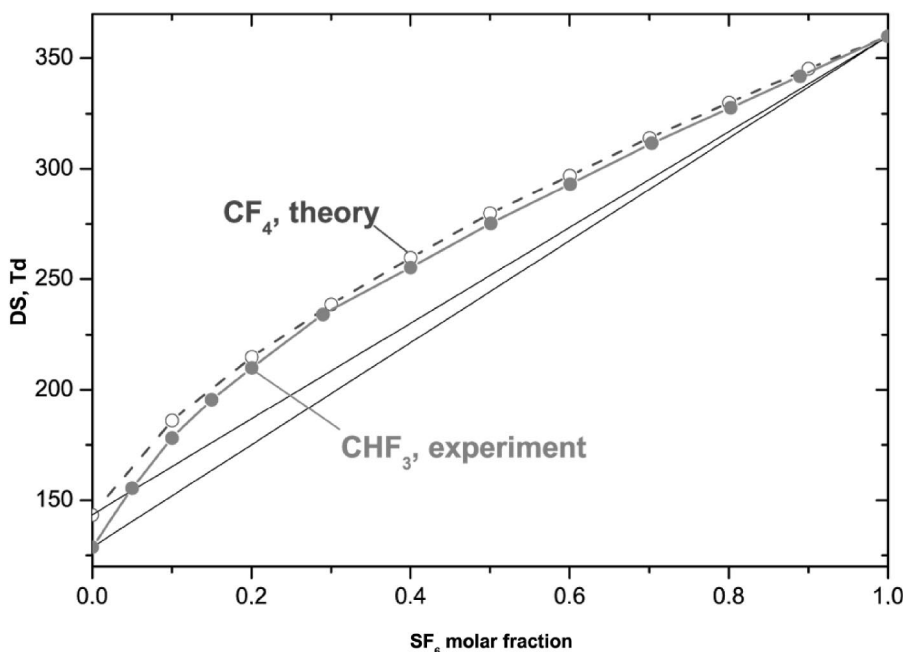


FIG. 3. Calculated dielectric strength (circles, in Td, 1 Td = 10^{-17} V cm²) in SF_6/CF_4 mixtures vs the SF_6 fraction (the relative DS increase is given in Table IV). Experimental data (filled signs) (Ref. 23) are recalculated considering that $DS(SF_6)$ is 360.1 Td and $DS(CHF_3)$ is 128.9 Td (Ref. 24).

TABLE V. Experimental relative dielectric strength (DS) increase^a and reduced electric field $(E/N)_{cr}$ values in the SF_6/CHF_3 mixture.

% SF_6	5	10	15	20	30	40	50.1	60.1	70.3	80.2	88.9	100
% DS	10.8	17.3	19.5	19.9	19.5	15.4	12.5	9.5	6.9	4.3	2.2	0.0
$(E/N)_{cr}$	155.5	178.2	195.4	209.8	234.1	255.4	275.3	293.2	311.5	327.7	341.8	360.1

^aAdapted from $(E/P)_{lim}$ values (Ref. 23) considering that the $DS(SF_6)=360.1$ Td and $DS(CHF_3)=128.9$ Td (Ref. 24); the experimental $(E/P)_{lim}$ value in pure CHF_3 was extrapolated by using a ninth-order polynomial fitting over 12 experimental points.

loss channels determine the synergism phenomenon. Additionally, this example shows that we deal with reciprocal changes of the rate constants of both the components and not with the variation of only one of them.

A difference between the WRC values of the ionization SF_6 and CF_4 channels is noted. The ionization WRC term of SF_6 becomes important at small CF_4 concentrations/high $(E/N)_{cr}$, i.e., right of Fig. 4, while the ionization WRC of CF_4 present a maximum.

ditions could be visualized by the differences between the rate constants in the mixture and in the pure gas submitted to the same reduced electric field $(E/N)_{cr}$ as shown in Fig. 5. Negative values of the $(k_{sj}(\text{mixture})-k_{sj}(s=S F_6 \text{ or } C F_4))$ differences mean that the j process is suppressed in the mixture as compared to the pure gas subject to the same $(E/N)_{cr}$. Namely, this behavior is revealed by the DN and ionization channels of CF_4 [Fig. 5(a)]. The WRC values of both processes are characterized by a maximum at the con-

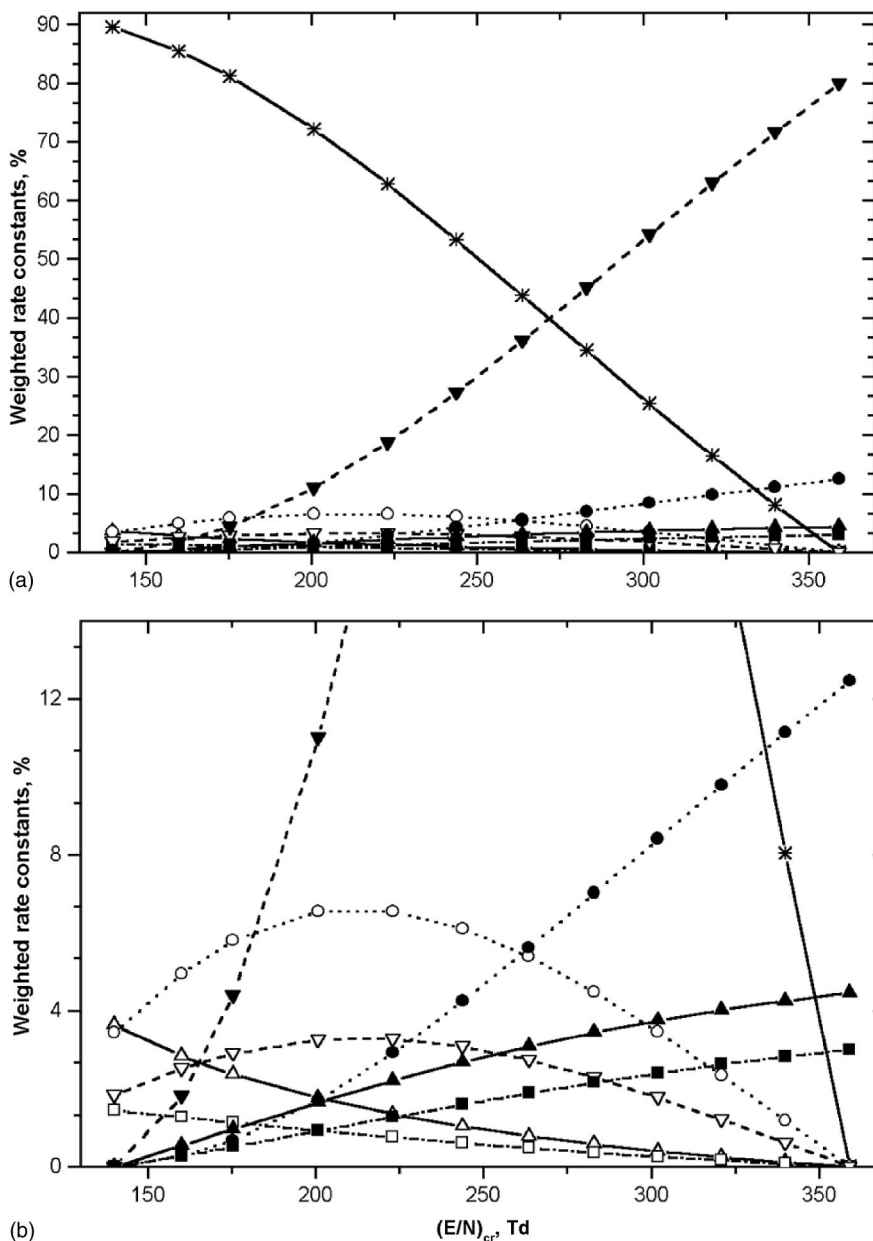


FIG. 4. Weighted rate constants (WRC) in the SF_6/CF_4 mixture vs the reduced critical electric field (respective mixture content is given in Table IV). WRC of vibration, dissociation into neutral particles, attachment, and ionization channels for both SF_6 (closed symbols) and CF_4 (open symbols) are shown by solid lines (vibration indirect by stars and vibration direct or vibration total by triangles up), dashed lines (triangles down), dotted-dashed lines, and dotted lines (circles), respectively: (a) full scale (top), and (b) detailed presentation (bottom).

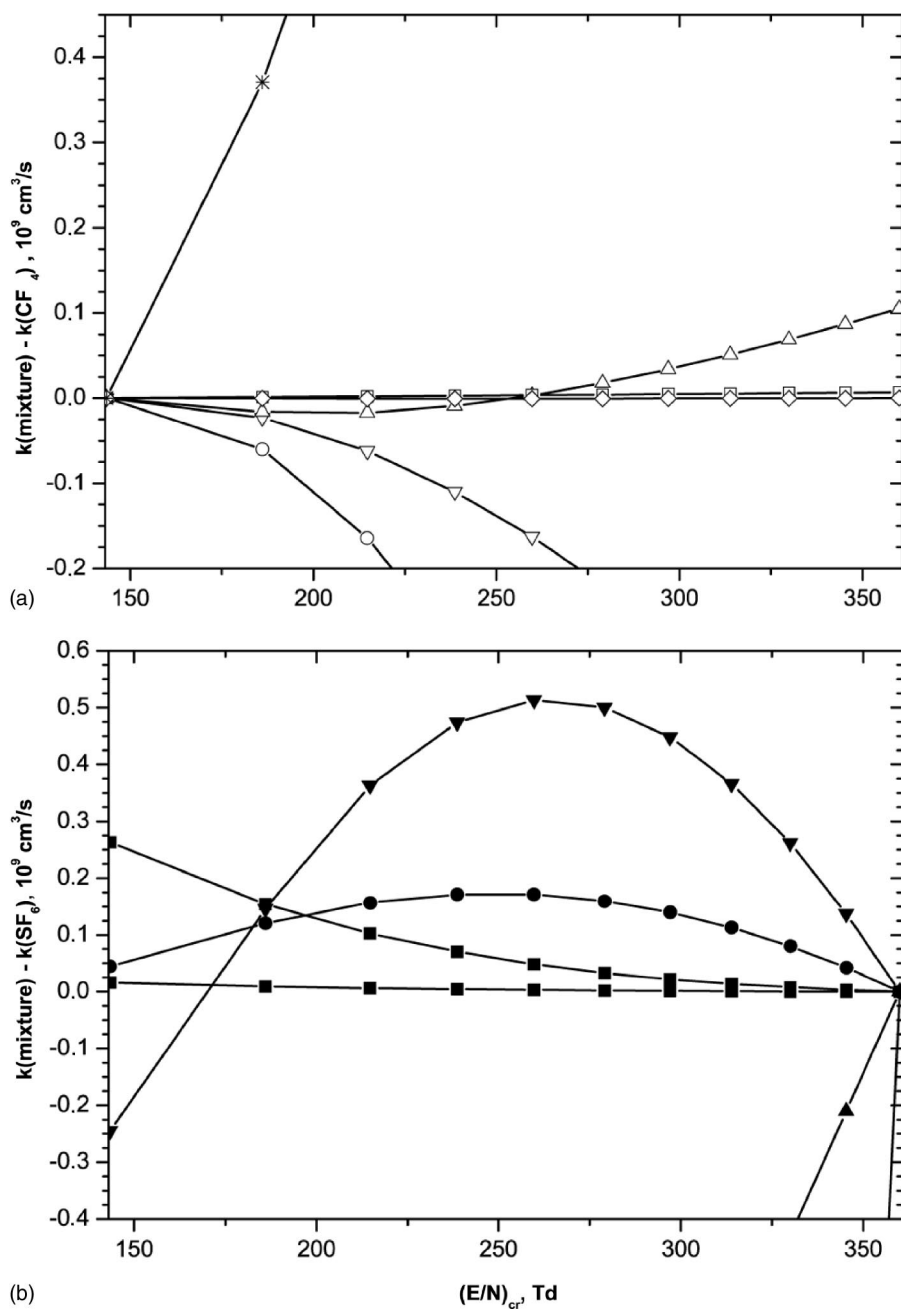


FIG. 5. Difference between the rate constants in the SF₆/CF₄ mixture and (a) CF₄ (top, open symbols) and (b) SF₆ (bottom, closed symbols) pure gases vs the reduced critical electric field (mixture contents are given in Table IV). Symbol notation corresponds to the one in Fig. 4. Two attachment (lower) and dissociative attachment (upper) channels are given for SF₆.

tent of 20 mol% or 214.7 Td (Table IV), which is close to that of the DS maximum. Surprisingly, the same $(k_i(\text{mixture}) - k_i(\text{SF}_6))$ differences for DN, dissociative attachment (DA), and ionization are positive [Fig. 5(b)], which signifies a higher effectiveness of these processes in the mixture as compared to pure SF₆ at the same $(E/N)_{cr}$ value. But the difference of the DN rate constants changes sign at nearly 170 Td, thus the DN of SF₆ diminishes the DS of the mixture below the $(E/N)_{cr}$ value [Fig. 5(b)]. Higher SF₆ ionization is compensated by the simultaneous DN increase for $(E/N)_{cr} > 170$ Td and by the DA increase for $(E/N)_{cr} < 170$ Td.

Varying the CS scaling factor, it is evidently possible to obtain a slightly different set of factors in agreement with the experimental ones. We verified the possible variations of the differences of the rate constants between the mixture and the pure gas and observed their “qualitative” stability. The nega-

tive $(k_{sj}(\text{mixture}) - k_{sj}(\text{CF}_4))$ differences and positive $(k_{sj}(\text{mixture}) - k_{sj}(\text{SF}_6))$ differences are conserved even at sharper variations of the rate constants, e.g., when the calculated DS increase is only around 9% at the same content of 20 mol% of SF₆. Such case can occur by using, for example, sets 2 of the CS scaling factors for both gases (Table I). These CSs result in closer electron drift velocities in the gases, 1.104 and 1.638×10^7 cm/s (Table II). The most drastic variation while shifting from CS set 1 to set 2 then corresponds to the DN channel of SF₆ whose maximum decreases up to 1.6×10^{-10} cm³/s while the DN curve intersects the abscissa at 200 Td instead of 170 Td. The ionization of SF₆ diminishes up to 9×10^{-11} cm³/s, whereas the constants of CF₄ remain nearly the same. Consequently, CS set 1 corresponds essentially to an higher increase of the

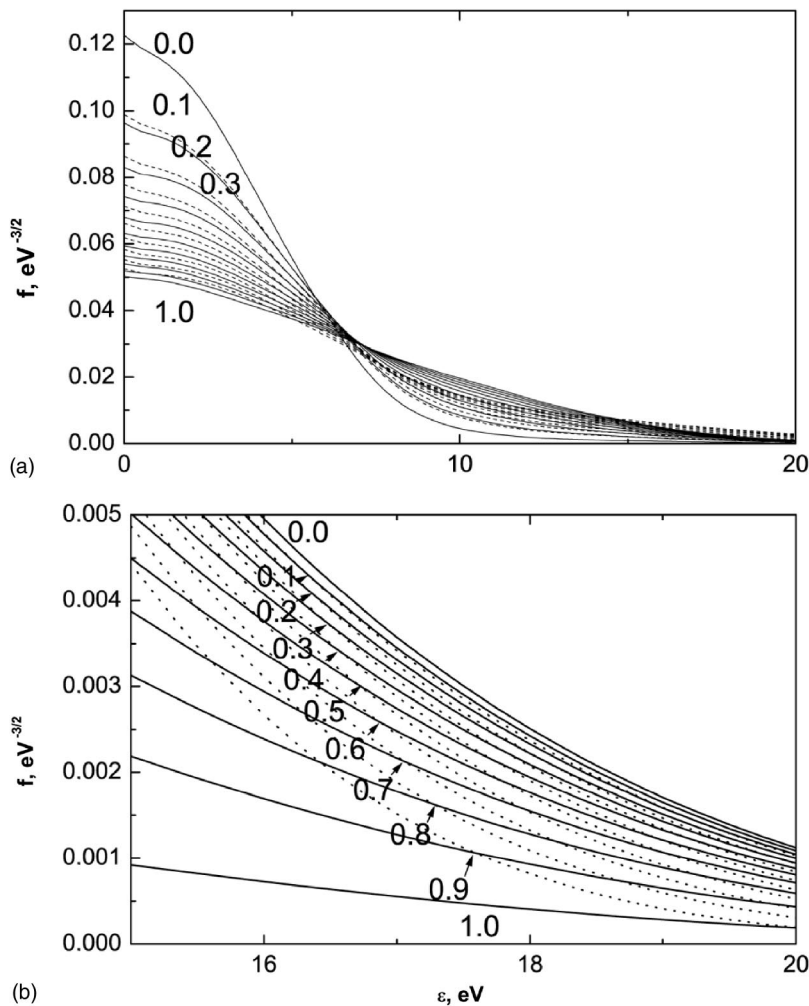


FIG. 6. Calculated electron energy distribution function (EEDF) for the SF_6/CF_4 mixture (solid lines) and (a) pure CF_4 (dashed lines) or (b) pure SF_6 (dotted lines) vs the electron energy under the same E/N values as given in Table IV. The crossing points between the EEDF of the SF_6/CF_4 mixture and the ones in pure SF_6 are shown by arrows in (b) with the SF_6 molar fraction labeling the lines.

DS due to the DN channel contribution of SF_6 . Despite the lower DS synergism with the CS set 2 for both components, its maximum position remains the same as observed in the calculations with CSs set 1.

IV. DISCUSSION

The general reasons of the DS synergism in binary gaseous mixtures seem to have probabilistic origins. A superposition of the total CSs of two different gases will rarely result in an exact coincidence of the “pits” in the CSs as for two Townsend minimum of each of the components at the same electron energy. Then this electron energy range of the coincident pits becomes a weak point of the mixture. This last situation is so rare that one cannot even cite one mixture for which all experimental data agree for a “negative” DS synergism. For example for $\text{C}_2\text{F}_6/\text{N}_2$, one citation reveals a negative synergism²⁷ while a positive synergism is reported in Ref. 28.

The well known CSs for the SF_6/CF_4 mixture components studied above allow to exclude such coincidence of the CS pits and the synergism is the logical consequence. Considering only one pair of gases as analyzed herein, one cannot provide a completely sure answer but one can suggest reasons for the asymmetric location of the maximum and hence propose a way for future verifications. The suppressed

CF_4 ionization and increased SF_6 ionization in the mixtures relative to pure CF_4 and SF_6 , respectively, at the same $(E/N)_{\text{cr}}$ values could explain the asymmetric position of the “maximum” of the relative DS increase (Table IV, Fig. 3). The evolution of the electron energy distribution function (EEDF) with the content and (E/N) explains why the SF_6 ionization is not suppressed at least at the higher SF_6 concentrations [solid lines in Figs. 6(a) and 6(b)]. The EEDF tail which grows up with the SF_6 molar fraction “opens” most of the channels with thresholds above 10 eV, i.e., ionization, DN,.... The difference between these tails of the EEDF in the mixture (solid lines) and pure CF_4 subject to the same E/N field [dashed lines in Fig. 6(a)] can illustrate the negative differences of the DN and ionization constants of CF_4 . If the EEDFs in pure CF_4 are slightly below the mixture functions within 10–15 eV, they become higher at energies above 15 eV, which is more important for the DN and ionization channels. On the contrary, the EEDFs in pure SF_6 become lower than the mixture functions [on the right starting from the points indicated by arrows in Fig. 6(b)]. This could be the reason of the shift of the relative DS maximum to small SF_6 concentrations where CF_4 ionization is suppressed. Such behavior means that the mixture is more stabilized with respect to the breakdown at smaller SF_6 concentrations. Hence, the link between the simultaneous opposite/

consistent variations of the ionizations of both components in other mixtures relative to their gas components should be traced to further confirm the asymmetric/symmetric displacement of the relative DS maximum relative to the 50% concentration.

V. CONCLUSIONS

Within the scope of the two-term approximation of Boltzmann equation corresponding to the model of an homogeneous electric field, we propose a way to calculate the dielectric strength (DS) for SF₆/CF₄ mixtures of various ratios. To do so, cross sections of all relevant electron–molecule processes in SF₆ and CF₄ were first scaled to simulate the experimental DS, attachment and ionization coefficients, as well as the electron drift velocities for the individual gases at the same theory level. Then, we succeeded to get a good agreement between the calculated DS for SF₆/CF₄ and the experimental data for SF₆/CHF₃. Via our theoretical models, we also allowed to assign the synergism in the SF₆/CF₄ mixture (i.e., the situation when the DS value at any content is simply larger than the value obtained by the linear interpolation between the values of the two pure gases at this content) to higher energy losses via dissociation into neutral particles of SF₆ and vibrational indirect excitations of CF₄ relative to the pure gases subject to the same reduced electric field. Our theoretical results clearly suggest that the asymmetric location of the DS maximum vs the mixture content is related to the suppressed CF₄ ionization and to the increased SF₆ ionization in the mixtures relative to pure CF₄ and SF₆.

ACKNOWLEDGMENTS

The authors are grateful to the European Commission for financial support in the framework of the COST Project No. ENK6-CT-2000-00087. They also thank most COST consortium members: Dr. F. Gentils (Schneider Electric, Grenoble, France), Dr. H.-J. Belt (Solvay, Hannover, Germany), Dr. E. Sandré, Dr. A. Aslanides (EDF, Moret sur Loing, France), and Dr. G. Rizzi, Dr. A. Caizzi, Dr. M. De Nigris (CESI, Milan, Italy) for fruitful discussions. A.V.L. acknowledge Professor J. Lowke (CSIRO, Australia) for useful advices regarding the dielectric strength calculations. Finally, N.M. thanks the “Fonds National de la Recherche Scientifique” for her Scientific Research Worker position.

- ¹S. R. Hunter and L. G. Christophorou, *J. Appl. Phys.* **57**, 4377 (1985).
- ²J. M. Wetzer and C. Wen, in *Gaseous Dielectrics VI*, edited by L. G. Christophorou and I. Sauers (Plenum, New York, 1991), p. 73.
- ³J. P. Novak and M. F. Fréchette, *J. Appl. Phys.* **55**, 107 (1984).
- ⁴L. G. Christophorou and J. K. Olthoff, *J. Phys. Chem. Ref. Data* **28**, 967 (1999).
- ⁵L. G. Christophorou and J. K. Olthoff, *J. Phys. Chem. Ref. Data* **29**, 267 (2000).
- ⁶A. Wieland, *ETZ, Elektrotech. Z., Ausg. A* **94**, 370 (1973).
- ⁷P. J. Chantry and R. E. Wootton, *J. Appl. Phys.* **52**, 2731 (1981).
- ⁸L. E. Kline, D. K. Davies, C. L. Chen, and P. J. Chantry, *J. Appl. Phys.* **50**, 6789 (1979).
- ⁹T. Yoshizawa, Y. Sakai, H. Tagashira, and S. Sakamoto, *J. Phys. D* **12**, 1839 (1979).
- ¹⁰M. Yousfi, P. Ségur, and T. Vassiliadis, *J. Phys. D* **18**, 359 (1985).
- ¹¹H. Itoh, Y. Miura, N. Ikuta, Y. Nakao, and H. Tagashira, *J. Phys. D* **21**, 922 (1988).
- ¹²H. Itoh, T. Matsumura, K. Satoh, H. Date, Y. Nakao, and H. Tagashira, *J. Phys. D* **26**, 1975 (1993).
- ¹³W. Pfeiffer, L. Z. Tong, and D. Schoen, in *Gaseous Dielectrics IX*, edited by L. G. Christophorou and J. K. Olthoff (Kluwer Academic/Plenum, New York, 2001), p. 135.
- ¹⁴M. C. Bordage, P. Ségur, and A. Chouki, *J. Appl. Phys.* **80**, 1325 (1996).
- ¹⁵A. V. Phelps and R. J. Van Brunt, *J. Appl. Phys.* **64**, 4269 (1988).
- ¹⁶G. A. Hebner and P. A. Miller, *J. Appl. Phys.* **87**, 7660 (2000).
- ¹⁷R. M. Thomson, K. Smith, and A. R. Davies, *Comput. Phys. Commun.* **11**, 369 (1976).
- ¹⁸S. D. Rockwood and A. E. Greene, *Comput. Phys. Commun.* **19**, 377 (1980).
- ¹⁹W. L. Morgan and B. M. Penetrante, *Comput. Phys. Commun.* **58**, 127 (1990).
- ²⁰W. H. Press, B. P. Flannery, S. A. Teukolsky, and W. T. Wetterling, *Numerical Recipes* (Cambridge University Press, New York, 1988).
- ²¹In lines 2008–2292 of the code, there is no common block/CERD/ containing the parameter NCALL, which defines the next step at line 2090 in the mode of the computations “with repeating data sets.” One of the authors (W.I.M.) of the code was informed.
- ²²M. C. Bordage, P. Ségur, L. G. Christophorou, and J. K. Olthoff, *J. Appl. Phys.* **86**, 3558 (1999).
- ²³J. Berril and I. W. McAllister, in *Gaseous Dielectrics VI*, edited by L. G. Christophorou and I. Sauers (Plenum, New York, 1991), p. 193.
- ²⁴A. K. Vijn, *IEEE Trans. Dielectr. Electr. Insul.* **EI-17**, 84 (1982).
- ²⁵O. Farish, *XVI Int. Conf. Phenom. Ioniz. Gases*, edited by W. Bötticher, H. Wenk, and E. Schulz-Gulde (Düsseldorf, 1983), p. 187.
- ²⁶E. Kuffel and K. Toufani, in *Gaseous Dielectrics VIII*, edited by L. G. Christophorou and J. K. Olthoff (Kluwer Academic/Plenum, New York, 1998), p. 197.
- ²⁷T. Yamada, T. Ishida, N. Hayakawa, S. Yuasa, S. Okabe, and H. Okubo, in *Gaseous Dielectrics IX*, edited by L. G. Christophorou and J. K. Olthoff (Kluwer Academic/Plenum, New York, 2001), p. 239.
- ²⁸Li Zheng-Ying and C. Zhang, in *Gaseous Dielectrics VII*, edited by L. G. Christophorou and D. R. James (Plenum, New York, 1994), p. 177.